2023 9th International Conference on Computer and Communications

Drone-assisted Communication for Traffic Load Balancing: Air-Ground Collaborative Perspective

Weihao Sun
College of Communications Engineering
Army Engineering University of PLA
Nanjing, China
imx_101@163.com

Hai Wang *
College of Communications Engineering
Army Engineering University of PLA
Nanjing, China
hai_wang@189.cn

2023 9th International Conference on Computer and Communications (ICCC) | 979-8-3503-1725-1/23/$31.00 ©2023 IEEE | DOI: 10.1109/ICCC59590.2023.10507278

***Abstract*—This paper studies the Air-Ground Collaborative Traffic Load Balancing (AGC-TLB) problem. Under such a setup, user equipment sets (UEs) perform different tasks requiring different data rates, and the macro base station (MBS) collaborates with several drone base stations (DBSs) to balance the network load condition. The user association and DBSs deployment are jointly optimized. We formulate the AGC-TLB problem as a generalized α-fairness minimization problem. Different load balancing degrees can be achieved with different coefficients α. The studied problem is a mixed-integer nonlinear programming (MINLP) problem that is challenging to be solved. To address this problem, an alternating optimization algorithm is developed. Specifically, the user association is solved by penalty-based successive convex approximation (P-SCA), whereas the DBSs deployment is modeled as an exact potential game. We analyze the existence of Nash equilibrium and propose the constrained Gibbs-sampling algorithm. Simulation results demonstrate that the proposed algorithm can achieve a load-balanced network condition compared to benchmark algorithms.**

***Index Terms*—Drone base station (DBS), traffic load balancing, QoS requirements, game theory.**

I. Introduction

With the advancement of Internet-of-Things (IoTs), the ever-growing and inhomogeneous traffic demands place a heavy load on the macro base station (MBS), resulting in a longer queue latency and lower throughput [1]. Thanks to the nature of flexible mobility and high-quality air-to-ground (A2G) links, drone base stations (DBSs) can be integrated into the cellular network to provide relay service, potentially improving load distribution. Accordingly, a natural problem arises: how to coordinate the MBS and DBSs to efficiently utilize network resources and achieve well-balanced traffic load conditions.

Traffic load condition, also known as the utilization of base station (BS) or the fraction of time the BS is active, is a paramount network metric [2]. Consider the stochastic traffic demands, in which the packets are randomly generated and then leave the system after transmission. The imbalanced load distribution creates a condition where the heavily loaded BSs experience congestion while others are underutilized.

Drone-assisted communication provides design freedom for on-demand deployment. To date, various literature exists on the DBSs deployment problems. In [3]–[7], the authors explored heuristic methods to improve the network performance involving the smallest enclosing circle, Voronoi partition, K-means clustering, weighted K-means clustering, and virtual force techniques. However, the quality of the backhaul link is ignored. The DBSs deployment exists a balance to strike since the favorable access links may come at the cost of the backhaul links, which eventually restricts the overall performance. In [8] and [9], the authors investigated the relay deployment problem and proposed online learning and Gibbs-sampling methods to maximize the network capacity and achieve traffic fairness, respectively. Note that user equipment sets (UEs) perform different tasks requiring different data rates. The ignorance of inhomogeneous demands also gives rise to unbalanced network load conditions.

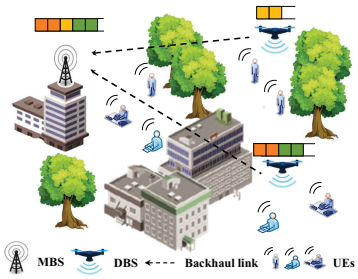

Fig. 1. Air-ground collaborative traffic load balancing scenario.

Compared with the existing efforts, our contributions are as follows: 1) the air-ground collaborative traffic load balancing (AGC-TLB) problem is investigated. We formulate the AGC-TLB problem as a generalized α-fairness minimization problem while accounting for the spatially inhomogeneous traffic demands. Different coefficients α come to different objective functions and enable to achieve different load balancing degrees. 2) we develop an alternating optimization algorithm to achieve a suboptimal solution. Concretely, the user association subproblem is solved by the penalty-based successive convex approximation (P-SCA), whereas the DBSs deployment subproblem is solved by the constrained Gibbs-sampling method. Numerical results verify the effectiveness of the proposed algorithm.

This work was supported by the National Natural Science Foundation of China under Grant 62171465. (*Corresponding author: Hai Wang.*)

II. System Model and Problem Formulation

As depicted in Fig.1, consider an uplink network with one MBS, multiple DBSs and UEs, where DBSs act as relays forwarding the data to the MBS. Specifically, UEs can upload their data towards the MBS directly or via the DBS relay. The set of UEs and DBSs are denoted by $\mathcal{I} = \{1, 2, ..., I\}$ and $\mathcal{J} = \{1, 2, ..., J\}$. In the Cartesian coordinate system, the 3D location of MBS s, UE i, and DBS j are denoted by $q_s = \{x_s, y_s, h_s\}$, $q_i = \{x_i, y_i, 0\}$, and $q_j = \{x_j, y_j, h_j\}$, respectively. We also denote the BS (DBSs and MBS) set as $\mathcal{J}^s = \mathcal{J} \cup \{s\}$. Assume that the orthogonal frequency division multiple access (OFDMA) technique is employed to realize interference alleviation as [3], [6], [9]. The proposed scheme can also be combined with the cognitive channel allocation mechanism as [8], [10]. Additionally, both the access and backhaul links share the same channel resource. To facilitate presentation, define the indicator variable $x_{i,j}$, where $x_{i,j} = 1$ if UE i associates to BS $j, j \in \mathcal{J}^s$.

A. Channel Model

1) Path loss from UE to DBS: The widely used probabilistic A2G channel model is employed to quantify the path loss [11]. The probability of line-of sight (LoS) link is given as,

$$P_{LoS}(\theta_{ij}) = \frac{1}{1+b_1 \exp(-b_2(\theta_{ij}-b_1))}, \tag{1}$$

where b_1 and b_2 are environmental parameters. $\theta_{ij} = \sin^{-1}(h_i/d_{ij})$ is the elevation angle between UEs i and DBS j, in which d_{ij} is the related distance. The probability of non-line-of-sight (NLoS) link is $P_{NLoS}(\theta_{ij}) = 1 - P_{LoS}(\theta_{ij})$. The path loss between UE i and DBS j is given as (unit:dB):

$$L_{ij} = P_{LoS}(\theta_{ij}) L_{ij}^{LoS} + P_{NLoS}(\theta_{ij}) L_{ij}^{NLoS}, \tag{2}$$

where L_{ij}^{LoS} and L_{ij}^{NLoS} are the path loss under the LoS and NLoS links as follows,

$$\begin{cases} L_{ij}^{LoS} = 20\log(4\pi f_c d_{ij}/c) + \zeta_{LoS}, \\ L_{ij}^{NLoS} = 20\log(4\pi f_c d_{ij}/c) + \zeta_{NLoS}, \end{cases} \tag{3}$$

where ζ_{LoS} and ζ_{NLoS} are the average additional path loss under LoS and NLoS links, respectively. f_c is the carrier frequency and c is the speed of electromagnetic wave. The channel gain can be indicated as $g_{ij} = 10^{-L_{ij}/10}$.

2) Path loss from DBS to MBS: The antennas of MBS are lifted from the ground in general. It is reasonably assumed that the LoS connection dominates the link from DBS to MBS [6]. The channel gain is given as,

$$g_{sj} = 10^{-L_{sj}^{LoS}/10}, \tag{4}$$

3) Path loss from UE to MBS: Since MBS and UEs are ground nodes, the A2G channel may be inappropriate. We employ the generalized channel model to quantify the path loss as [8], which is given by ,

$$g_{is} = \delta d_{is}^{-\kappa}, \tag{5}$$

where δ denotes the unit channel gain. d_{is} is the related distance, in which κ denotes the path loss exponent.

B. Achievable Data Rate Model

Denote γ_{is} as the signal-to-noise ratio from UE i to MBS s. The achievable data rate from MBS s is given as,

$$r_{is} = W_s \log(1 + \gamma_{is}), \tag{6}$$

where W_s is the bandwidth of MBS s.

Apart from the direct transmission, UEs can also upload the data via the DBS relay. For the cooperative communication model, we employ the amplify-and-forward (AF) relay mode. Specifically, the transmission process is divided into two phases. The first phase is used for transmission from UE i towards the MBS s and DBS j. The second phase is relay forwarding from the DBS j towards the MBS s. According to [12], the achievable data rate of UE i from DBS j is given as,

$$r_{ij} = \frac{W_j}{2} \log_2 \left(1 + \gamma_{is} + \frac{\gamma_{ij}\gamma_{sj}}{1 + \gamma_{ij} + \gamma_{sj}}\right), \tag{7}$$

where γ_{ij} and γ_{sj} denote the signal-to-noise ratio from UE i to DBS j and DBS j to MBS s, respectively.

C. Traffic Load Model

Assume that the packets generated at UE i follows the Poisson distribution with the rate λ_i. Meanwhile, the packet sizes are independently distributed with mean μ. The average traffic load of BS j is given as,

$$\varrho_j = \sum_{i \in \mathcal{I}} \frac{x_{ij}\lambda_i \mu}{r_{ij}}. \tag{8}$$

where $\varrho_j \in [0, 1]$ also indicates the utilization or the fraction of time the BS is active. The traffic load balancing problem in general revolves around different load policies with specific load balancing degrees. Inspired by [2], we formulate the BSs' load distribution as an α-fairness minimization problem,

$$\min \phi_\alpha(\varrho) = \begin{cases} \sum\limits_{j \in \mathcal{J}^s} \frac{(1-\varrho_j)^{1-\alpha}}{\alpha - 1}, & \alpha \geq 0, \alpha \neq 1, \\ -\sum\limits_{j \in \mathcal{J}^s} \log\left(1 - \varrho_j\right), & \alpha = 1. \end{cases} \tag{9}$$

where $1 - \varrho_j$ denotes the BS's idle time. The α-fairness function specifies the load balancing degrees with different coefficients α [13]. **Min-sum load policy ($\alpha = 0$):** $\phi_\alpha(\varrho) = -\sum_{j \in \mathcal{J}^s}(1 - \varrho_j)$. Minimizing $\phi_\alpha(\varrho)$ equals to maximize the sum of BSs' idle time, equivalently as minimizing the sum of BSs' traffic load. **Proportional-fair policy ($\alpha = 1$):** $\phi_\alpha(\varrho) = -\sum_{j \in \mathcal{J}^s} \log(1 - \varrho_j) = -\log \prod_{j \in \mathcal{J}^s}(1 - \varrho_j)$. Minimizing $\phi_\alpha(\varrho)$ equals to achieve proportional-fair performance or maximize the geometric mean of BS's idle time. **Latency-optimal policy ($\alpha = 2$):** $\phi_\alpha(\varrho) = \sum_{j \in \mathcal{J}^s} \frac{1}{1-\varrho_j}$. Minimizing $\phi_\alpha(\varrho)$ equals to maximize the harmonic mean of BSs' idle time. Following the queue theory, the Little's formula indicates that average latency in an M/G/1/PS system is $\sum_{j \in \mathcal{J}^s} \frac{\varrho_j}{1-\varrho_j} = \sum_{j \in \mathcal{J}^s}(\frac{1}{1-\varrho_j} - 1)$, which is the latency-optimal policy. **Min-max load policy ($\alpha = +\infty$):** $\phi_\alpha(\varrho) = \sum_{j \in \mathcal{J}^s} \frac{(1-\varrho_j)^{1-\alpha}}{\alpha - 1}$. As α increases, the indication of $\phi_\alpha(\varrho)$ shifts from network efficiency toward load equalization. Minimizing $\phi_\alpha(\varrho)$ equals to

maximize the min BSs' idle time, equivalently as minimizing the max BSs' load condition.

Define $\mathbf{Q} := \{q_j, j \in \mathcal{J}\}$ and $\mathbf{X} := \{x_{ij}, i \in \mathcal{I}, j \in \mathcal{J}^s\}$. The investigated AGC-TLB problem can be formulated as,

$$\min_{\mathbf{Q},\mathbf{X}} \quad \phi_\alpha(\varrho) \tag{10a}$$

$$\text{s.t.} \sum_{j\in\mathcal{J}^s} x_{ij} = 1,\ x_{ij} \in \{0,1\},\ \forall i \in \mathcal{I}, \tag{10b}$$

$$\sum_{i\in\mathcal{I}} x_{ij} \le N_j,\ \forall j \in \mathcal{J}^s, \tag{10c}$$

$$0 \le \varrho_j \le \varrho_{max},\ \forall j \in \mathcal{J}^s, \tag{10d}$$

$$q_j \in \mathcal{F},\ \forall j \in \mathcal{J}. \tag{10e}$$

Constraint (10b) indicates that each UE is associated to one BS. Constraint (10c) ensures that the number of associated UEs of BS j cannot exceed the max quota. Constraint (10d) imposes the traffic load threshold to ensure network stability. Constraint (10e) is the feasible deployment region $\mathcal{F} = [x_{min}, x_{max}] \times [y_{min}, y_{max}] \times [h_{min}, h_{max}]$. The formulated problem is a mixed-integer nonlinear programming (MINLP) problem with NP-hard complexity [6]. In the following, we will propose an alternating optimization algorithm to achieve a sub-optimal solution.

III. Proposed Solution

A. User Association Subproblem

For given DBS deployment, we optimize the user association subproblem. To tackle the binary variable $x_{i,j}$, we relax x_{ij} into $\tilde{x}_{ij}, 0 \le \tilde{x}_{ij} \le 1$. Since $\tilde{x}_{ij} \ge \tilde{x}_{ij}^2$, (10b) is equivalent to the following intersection region,

$$\sum_{j\in\mathcal{J}^s} \tilde{x}_{i,j} = 1, 0 \le \tilde{x}_{i,j} \le 1,\ \ \forall i \in \mathcal{I}, \tag{11}$$

$$\sum_{i\in\mathcal{I}} \sum_{j\in\mathcal{J}^s} (\tilde{x}_{ij} - \tilde{x}_{ij}^2) = 0. \tag{12}$$

To proceed, we employ the penalty-based strategy. The key idea is to add a penalty term to the objective function if the binary constraint is violated. Formally,

$$\min_{\tilde{x}_{ij}} \quad \phi_\alpha(\varrho) + \frac{1}{\lambda} \sum_{i\in\mathcal{I}} \sum_{j\in\mathcal{J}^s} (\tilde{x}_{ij} - \tilde{x}_{ij}^2) \tag{13a}$$

$$\text{s.t.} \sum_{j\in\mathcal{J}^s} \tilde{x}_{i,j} = 1,\ 0 \le \tilde{x}_{i,j} \le 1,\ \forall i \in \mathcal{I}, \tag{13b}$$

$$(10c),\ \ (10d). \tag{13c}$$

where $\lambda > 0$ is a penalty parameter. Although x_{ij} is relaxed, when $\lambda \to 0$ or $1/\lambda \to +\infty$, the obtained solution is exactly the feasible solution of original problem. Regarding (13a), the penalty term $\tilde{x}_{ij} - \tilde{x}_{ij}^2$ is concave with respect to (w.r.t.) $\tilde{x}_{ij}$. By applying the first-order Taylor approximation, *i.e.*, $\tilde{x}_{ij} - \tilde{x}_{ij}^2 \le \tilde{x}_{ij} - {\tilde{x}_{ij}^f}^2 - 2\tilde{x}_{ij}^f(\tilde{x}_{ij} - \tilde{x}_{ij}^f)$, where $\tilde{x}_{ij}^f$ is the feasible point of $\tilde{x}_{ij}$, an upper-bound of problem (13) can be obtained $\phi_\alpha^{ub}(\varrho) := \phi_\alpha(\varrho) + \frac{1}{\lambda} \sum_{i\in\mathcal{I}} \sum_{j\in\mathcal{J}^s} (\tilde{x}_{ij} - {\tilde{x}_{ij}^f}^2 - 2\tilde{x}_{ij}^f(\tilde{x}_{ij} - \tilde{x}_{ij}^f))$. Thus, problem (13) can be rewritten as,

$$\min_{\tilde{x}_{ij}} \quad \phi_\alpha^{ub}(\varrho) \tag{14a}$$

$$\text{s.t.} \sum_{j\in\mathcal{J}^s} \tilde{x}_{i,j} = 1,\ 0 \le \tilde{x}_{i,j} \le 1,\ \forall i \in \mathcal{I}, \tag{14b}$$

$$(10c),\ \ (10d). \tag{14c}$$

Proposition 1: Problem (14) is a convex problem.

Proof: Without loss of generality, we take the second-order derivative of the $\phi_\alpha^{ub}(\varrho)$ w.r.t $\tilde{x}_{ij}$,

$$\frac{\partial^2 \phi_\alpha^{ub}(\varrho)}{\partial^2 \tilde{x}_{ij}} = \left(\frac{\lambda_i \mu_i}{r_{ij}}\right)^2 \frac{\alpha}{(1-\varrho_j)^{\alpha+1}}, \quad \forall \alpha \ge 0. \tag{15}$$

Since the second-order derivative is non-negative, $\phi_\alpha^{ub}(\varrho)$ is convex w.r.t $\tilde{x}_{ij}$. Besides, the feasible set is also a convex set. Thus, Problem (14) is a convex problem, and can be solved by optimization solver, such as CVX [14]. ■

In practical implementation, setting penalty parameter λ as a constant is undesirable since the objective function with a small λ will be dominated by the penalty term, ignoring the original objective. In contrast, a large λ decreases the penalty effect, violating the binary constraint. To tackle such difficulty, we adopt the double-loop penalty-based solution [15]. Concretely, we approximately solve the penalized problem (14) with a given λ in each inner loop. In the outer loop, we decrease the λ to increase the binary constraint until convergence as follows,

$$\lambda := \vartheta\lambda, \quad 0 \le \vartheta \le 1. \tag{16}$$

where ϑ is a scaling parameter. The load distribution can be well-balanced within a predefined accuracy while satisfying the binary constraint. Details are illustrated in Algorithm 1.

B. DBS Deployment Subproblem

For given user association, we optimize the DBS deployment subproblem. The hardness derives from that the complicated probabilistic A2G channel and AF relay model prohibit the use of standard convex or combinatorial optimization techniques. In this case, we first formulate the DBS deployment as an exact potential game. Then, we analyze the convergence and propose constrained Gibbs-sampling-based method.

To be specific, consider the discrete 3D grid, where $X = \{x_{min}, x_{min}+\delta_x, ..., x_{max}\}$, $Y = \{y_{min}, y_{min}+\delta_y, ..., y_{max}\}$ and $H = \{h_{min}, h_{min} + \delta_h, ..., h_{max}\}$ with δ_x, δ_y, and δ_h representing the grid granularity. Mathematically, the proposed game is denoted by $\mathcal{G} = \{\mathcal{J}, \mathcal{A}, \{\mathcal{C}_j\}_{j\in\mathcal{J}}\}$, wherein DBSs act as players. $\mathcal{A} = \prod_{j\in\mathcal{J}} \mathcal{A}_j$ is the strategy profiles of all players, where $\mathcal{A}_j = X \otimes Y \otimes H$ denotes the finite strategy of player j and '$\otimes$' is the Cartesian product. $\mathcal{C}_j$ is the individual cost function. Following the objective function (9), the cost function of player j is designed as,

$$\mathcal{C}_j(a_j, a_{-j}) = \begin{cases} \frac{(1-\varrho_j)^{1-\alpha}}{\alpha-1}, & \alpha \ge 0, \alpha \ne 1, \\ -\log(1-\varrho_j), & \alpha = 1. \end{cases} \tag{17}$$

where $a_j \in \mathcal{A}_j$ denotes the action of BS j, and a_{-j} denotes the actions of other BSs except DBS j, *i.e.*, $\{-j\} = \{\mathcal{J}^s \backslash j\}$.

Next, we analyze the convergence of proposed game. To facilitate presentation, we introduce the following definition.

Definition 1(Exact potential game (EPG) [16]): $\mathcal{G}$ is an exact potential game if there exists a potential function $\Phi(a_j, a_{-j})$ and cost function $\mathcal{C}(a_j, a_{-j})$ such that $\forall j \in \mathcal{J}$,

$$\Phi(a'_j, a_{-j}) - \Phi(a_j, a_{-j}) = \mathcal{C}_j(a'_j, a_{-j}) - \mathcal{C}_j(a_j, a_{-j}). \quad (18)$$

Proposition 2: The proposed game $\mathcal{G}$ is an exact potential game and will converge to a stable result.

Proof: We design the original objective function as the potential function,

$$\Phi(a_j, a_{-j}) = \mathcal{C}_j(a_j, a_{-j}) + \sum_{j' \in \mathcal{J}^s \backslash j} \mathcal{C}_{j'}(a_{j'}, a_{-j'}). \quad (19)$$

Suppose DBS j changes its action from a_j towards a'_j, the decrease of potential function is given by,

$$\begin{aligned} &\Phi(a'_j, a_{-j}) - \Phi(a_j, a_{-j}) \\ &= \mathcal{C}_j(a'_j, a_{-j}) - \mathcal{C}_j(a_j, a_{-j}) \\ &+ \sum_{j' \in \mathcal{J}^s \backslash j} \mathcal{C}_{j'}(a'_{j'}, a_{-j'}) - \sum_{j' \in \mathcal{J}^s \backslash j} \mathcal{C}_{j'}(a_{j'}, a_{-j'}). \end{aligned} \quad (20)$$

Since BSs operate in the orthogonal frequency bands, the actions profile (a'_j, a_{-j}) is independent of $\sum_{j' \in \mathcal{J}^s \backslash j} \mathcal{C}_{j'}(a_{j'}, a_{-j'})$. We have,

$$\sum_{j' \in \mathcal{J}^s \backslash j} \mathcal{C}_{j'}(a'_{j'}, a_{-j'}) - \sum_{j' \in \mathcal{J}^s \backslash j} \mathcal{C}_{j'}(a_{j'}, a_{-j'}) = 0. \quad (21)$$

Joint (17), (19), and (20) yields the following equation,

$$\Phi(a'_j, a_{-j}) - \Phi(a_j, a_{-j}) = \mathcal{C}_j(a'_j, a_{-j}) - \mathcal{C}_j(a_j, a_{-j}). \quad (22)$$

As per Eq.(22), the changes in the potential function are the same as the individual cost function, which verifies that the proposed game is an EPG. The existing effort [16] has proved that EPG exists at least one pure-strategy Nash Equilibrium. Thus, the proposed game will converge to a stable result. Proposition 2 holds. ■

The proposed constrained Gibbs-sampling-based deployment algorithm is given as follows. The key idea is to design a Markov chain to update the deployment scheme. At iteration t, DBSs successively consider the constrained strategy profiles $\mathcal{A}_j^t$, including the current location (x_j, y_j, h_j) and the neighboring locations, $(x_j \pm \delta_x, y_j, h_j)$, $(x_j, y_j \pm \delta_y, h_j)$, and $(x_j, y_j, h_j \pm \delta_h)$. DBS j selects an action $a_j^t, a_j^t \in \mathcal{A}_j^t$ and updates its location based on the state transfer probability,

$$\Pr(a_j^t | a_j^{t-1}) = \frac{\exp\{-\varpi \mathcal{C}_j(a_j^t, a_{-j}^t)\}}{\sum\limits_{a_j'^t \in \mathcal{A}_j^t} \exp\{-\varpi \mathcal{C}_j(a_j'^t, a_{-j}^t)\}}, \quad (23)$$

Algorithm 1 AGC-TLB algorithm

1: Initialize a feasible solution $(\mathbf{Q}, \mathbf{X})$, accuracy tolerance ϵ, and penalty parameter $\lambda = \lambda_{init}$. Set the iteration number $t = 0$.
2: **repeat**
3: **repeat**
4: Update $\mathbf{X}^{(t)}$ by solving problem (14) with given $\mathbf{Q}^{(t)}$.
5: Update $\lambda := \vartheta\lambda$.
6: **until** The objective value decreases below the threshold ϵ.
7: Update $\mathbf{Q}^{(t)}$ by the transfer probability (24) with given $\mathbf{X}^{(t)}$.
8: t = t + 1.
9: **until** The objective value decreases below the threshold ϵ or iteration reaches the maximal iteration number.

where $\varpi \geq 0$ is the Boltzmann parameter to balance the tradeoff between exploitation and exploration. In addition, since the first-order derivative of $\mathcal{C}_j(a_j, a_{-j})$ w.r.t. ϱ_j is non-negative, *i.e.*, $\partial \mathcal{C}_j / \varrho_j = (1 - \varrho_j)^{-\alpha}, \forall \alpha \geq 0$, the state transfer probability can be further simplified as,

$$\Pr(a_j^t | a_j^{t-1}) = \frac{\exp\{-\varpi \varrho_j(a_j^t, a_{-j}^t)\}}{\sum\limits_{a_j'^t \in \mathcal{A}_j^t} \exp\{-\varpi \varrho_j(a_j'^t, a_{-j}^t)\}}, \quad (24)$$

where $\varrho_j(a_j^t, a_{-j}^t)$ is the traffic load of DBS j w.r.t. action profile (a_j^t, a_{-j}^t).

Remark: As $\varpi \to +\infty$, the stationary distribution of DBS deployment converges. Mathematically,

$$\lim_{\varpi \to +\infty} \Pr(a_j^t = a_j^{*t} | a_j^{t-1}) = 1. \quad (25)$$

where $a_j^{*t} = \arg\min_{a_j^t \in \mathcal{A}_j{}^t} C(a_j^t, a_{-j}^t)$ indicates that the selected action always minimizes the individual cost function. Since the proposed game is an EPG, the objective function is also minimized and converges to a stable result.

C. Overall Algorithm

The proposed AGC-TLB algorithm is illustrated in **Algorithm 1**. The user association and DBSs deployment subproblems can solved by the P-SCA and constrained Gibbs-sampling techniques, respectively. The algorithm operates iteratively and alternatively, which terminates until the objective value decreases below a given threshold.

The computational complexity is analyzed as follows. In each iteration, the P-SCA algorithm has a complexity of $\mathcal{O}(I(J+1))^{3.5} \log^2(1/\epsilon)$ with the order of outer iterations given by $\mathcal{O}(\log 1/\epsilon)$ [15]. For DBSs deployment scheme, each DBS computes the individual cost function of all the possible states and selects the action based on the state transfer probability. Thus, the overall complexity is $\mathcal{O}(JK(IJ + I)^{3.5} \log^2(1/\epsilon)T)$, where T denotes the convergence of iteration number, and $K = |\mathcal{A}_j|$ is the cardinality of constrained strategy profile.

IV. Simulation Results

In this section, simulations are conducted to verify the effectiveness. Consider a system scenario where UEs are randomly distributed in a 1000*1000 m^2 task region. Each BS achieves 4MHz bandwidth exclusively. The transmission power of UEs and DBSs are set as 20 mW and 200 mW, respectively. Major

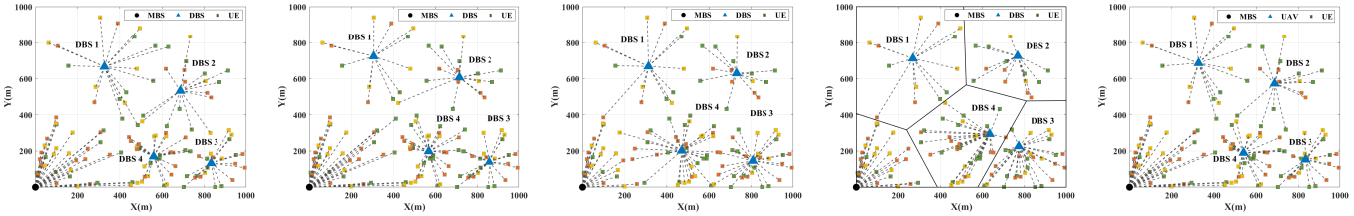

(a) AGC-TLB ($\alpha = 10$) (b) Latency-aware scheme (c) K-means scheme (d) Voronoi partition scheme (e) Traffic fairness scheme

Fig. 2. Network configuration with 4 DBSs and 1 MBS. Different colors indicate different packet generated rate of UEs. Red is 1.5 packets/s. Yellow is 1 packets/s and green is 0.5 packets/s, respectively. The average packet size is 100 KB.

parameters are given as follows [11]: $b_1 = 9.61$, $b_2 = 0.21$, $\zeta_{LoS} = 1$ dB, $\zeta_{NLoS} = 20$ dB, $\sigma^2 = -110$ dB, $h_{max} = 200$m, $\varrho_{max} = 1$, $\varpi = 1.3^t$, and $\kappa = 2$.

We consider the following benchmark algorithms, involving latency-aware (LA) scheme [6], K-means scheme [5], Voronoi partition (VP) scheme [4], and traffic fairness (TF) scheme [9]. Specifically, the VP scheme partitions the region into local Voronoi cells. The LA scheme deploys the DBSs at the weighted geometric center of traffic demands and then updates the user association to minimize the average latency. In the TF scheme, the DBSs deployment and user association are alternatively optimized with the Gibbs-sampling and fractional relaxation methods to maximize the minimum data rate

Fig. 2 and Fig. 3 show the network configurations and load distribution under different algorithms. We can observe that UEs around the MBS upload the data directly, while others upload via the DBS relay. In addition, due to ignoring the UEs' different data rate requirements, we note that the load condition of some BSs exceed the load threshold, which yields infeasible solution. According to the statistics, the proposed AGC-TLB algorithm achieves a load-balanced network condition and reduces the BSs' max load by 13%, 36%, 53% and 11%, compared with the LA scheme, K-means scheme, VP scheme, and TF scheme. This is expected since the LA, K-means, and VP algorithms' deployment scheme ignores the trade-off between the access and backhaul link quality, as well as the design freedom of 3D deployment. In the TF scheme, the heterogeneous demands of UEs fail to consider.

Fig.4 investigates the transmission delay versus the packet size, and the coefficient in the proposed scheme is set as $\alpha = 2$. When the packet size is small, the overall network load condition is light. The proposed scheme has a similar performance to the TF and LA schemes. However, as the packet size increases, the transmission delay of proposed scheme significantly improves compared with the benchmark algorithms. This simulation verifies the performance gain of the proposed scheme in the network with heavily-loaded condition.

Fig.5 studies the impact of grid granularity w.r.t. the instantaneous min-max load condition over iterations. The coefficient is set as $\alpha = 10$. The high resolution describes a grid with $20\times20\times10$ m^3 granularity, and the low resolution corresponds to a $100\times100\times20$ granularity. Notably, a high grid granularity

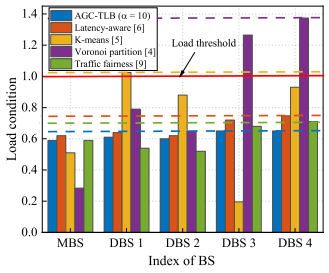

Fig. 3. Traffic load distribution.

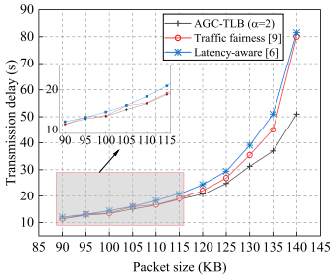

Fig. 4. Transmission delay versus packet size.

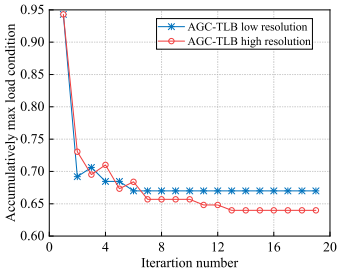

Fig. 5. Convergence behavior. The average packet size is 100 KB.

gives rise to accurate results. However, the large number of possible deployment schemes result in a longer convergence time. It is observed that the low-resolution granularity converges at a fast speed at the cost of accuracy. In contrast, the high-resolution granularity enables better performance with a slower convergence speed.

Finally, Table I presents the load metric versus different coefficients α, involving the sum load metric, proportional

TABLE I
LOAD METRIC VERSUS DIFFERENT α

	$\alpha=0$	$\alpha=1$	$\alpha=2$	$\alpha=10$
$\sum_{j\in\mathcal{J}^s}\varrho_j$	**2.94**	3.04	3.09	3.14
$-\sum_{j\in\mathcal{J}^s}\log(1-\varrho_j)$	5.27	**4.82**	4.87	4.96
$\sum_{j\in\mathcal{J}^s}(\frac{1}{1-\varrho_j})$	17.38	13.53	**13.40**	13.51
$\max\{\varrho_j\}_{j\in\mathcal{J}_s}$	0.85	0.72	0.68	**0.64**

fairness of BSs' idle time metric, harmonic mean of BSs' idle time metric, and the max load metric. As α increases, the indication of the objective function shifts from the network efficiency toward load equalization. We observe that the sum load metric increases with the coefficient α, whereas the max load metric decreases. This is because UEs accessing the BS providing the maximal data rate is efficient, yet it may give rise to an unbalanced load distribution. Similarly, transferring the traffic demands from overloaded BS toward the lightly loaded BS may sacrifice efficiency. In this case, we find that the sum load metric may increase. This simulation reveals the trade-off between efficiency and load balancing and also verifies the scalability.

V. CONCLUSION

This paper studied the air-ground collaborative traffic load balancing problem while accounting for the spatially inhomogeneous traffic demands. We formulated the traffic load balancing problem as a generalized α-fairness minimization problem. The user association and DBSs deployment problem were jointly optimized by penalty-based successive convex approximation and constrained Gibbs-sampling techniques. Numerical results demonstrated that the proposed algorithm could achieve a load-balanced network condition and outperform benchmark algorithms. We will extend the system model towards drone-assisted multi-hop routing in the future.

REFERENCES

[1] Y. Qu *et al.*, "Service provisioning for UAV-enabled mobile edge computing," *IEEE Journal on Selected Areas in Communications*, vol. 39, no. 11, pp. 3287–3305, 2021.

[2] H. Kim, G. de Veciana, X. Yang, and M. Venkatachalam, "Distributed α -optimal user association and cell load balancing in wireless networks," *IEEE/ACM Transactions on Networking*, vol. 20, no. 1, pp. 177–190, 2012.

[3] X. Luo *et al.*, "3D deployment of multiple UAV-mounted mobile base stations for full coverage of IoT ground users with different QoS requirements," *IEEE Communnications Letter*, vol. 26, no. 12, pp. 3009–3013, 2022.

[4] X. Liu *et al.*, "Distributed deployment in UAV-assisted networks for a long-lasting communication coverage," *IEEE System Journal*, pp. 1–9, 2021.

[5] B. S. H. El Hammouti, M. Benjillali and M. S. Alouini, "Learn-as-you-fly: A distributed algorithm for joint 3D placement and user association in multi-UAVs networks," *IEEE Transactions on Wireless Communications*, vol. 18, no. 12, pp. 5831–5844, Dec. 2019.

[6] Q. Fan and N. Ansari, "Towards traffic load balancing in drone-assisted communications for IoT," *IEEE Internet of Things Journal*, vol. 6, no. 2, pp. 3633–3640, 2019.

[7] S. G. L. Wang, H. Zhang and D. Yuan, "3D UAV deployment in multi-UAV networks with statistical user position information," *IEEE Communications Letters*, vol. 26, no. 6, pp. 1363–1367, 2022.

[8] N. L. X. Zhong, Y. Guo and Y. Chen, "Joint optimization of relay deployment, channel allocation, and relay assignment for UAVs-aided D2D networks," *IEEE/ACM Transactions on Networking*, vol. 28, no. 2, pp. 804–817, 2020.

[9] Z. Kang, C. You, and R. Zhang, "3D placement for multi-UAV relaying: An iterative gibbs-sampling and block coordinate descent optimization approach," *IEEE Transactions on Communications*, vol. 69, no. 3, pp. 2047–2062, 2021.

[10] D. Liu *et al.*, "Task-driven relay assignment in distributed UAV communication networks," *IEEE Transactions on Vehicular Technology*, vol. 68, no. 11, pp. 11 003–11 017, Nov. 2019.

[11] A. Al-Hourani, S. Kandeepan, and S. Lardner, "Optimal LAP altitude for maximum coverage," *IEEE Wireless Commun. Lett.*, vol. 3, no. 6, pp. 569–572, Dec. 2014.

[12] J. Laneman, D. Tse, and G. Wornell, "Cooperative diversity in wireless networks: Efficient protocols and outage behavior," *IEEE Transactions on Information Theory*, vol. 50, no. 12, pp. 3062–3080, 2004.

[13] J. Mo and J. Walrand, "Fair end-to-end window-based congestion control," *IEEE/ACM Transactions on Networking*, vol. 8, no. 5, p. 12, 2000.

[14] M. Grant and S. Boyd, "CVX: Matlab software for disciplined convex programming, version 2.1," http://cvxr.com/cvx, Mar. 2014.

[15] Q. Wu and R. Zhang, "Joint active and passive beamforming optimization for intelligent reflecting surface assisted swipt under qos constraints," *IEEE Journal on Selected Areas in Communications*, vol. 38, no. 8, pp. 1735–1748, 2020.

[16] D. Monderer and L. Shapley, "Potential games," *Games Econ. Behav.*, vol. 14, pp. 124–143, 05 1996.